Nanomaterials synthesis in combustion

Z.A. Mansurov

***Abstract*—** This paper presents original results in the area of synthesis of fullerenes, carbon nanotubes, graphene, and superhydrophobic soot in hydrocarbon flames and data on the self-propagating high- temperature synthesis of nanomaterials obtained in recent years at the Institute of Combustion Problems.

***Keywords*—** carbon nanotubes, fullerenes, graphene, nanomaterials.

I. Introduction

The practical use of combustion processes can be divided into two areas: energetic and chemical-technological. In the first case, use is made of the heat of combustion and very often, but not always, the energy of expanding gaseous products. In the second case, of interest is the combustion product itself, which is the target material of the chemical-technological process [1]-[5].

As regards the chemical-technological area, it has been developed in isolation from the theory of combustion, mostly by chemical engineers and metallurgists, and has reduced to the development of individual processes. Unfortunately, the scope and level of research are not high enough and are not adequate to the importance and relevance of this problem [4], [5].

The main feature of technological combustion processes is that the desired product is produced by a combustion reaction which proceeds spontaneously at high temperatures, at a high rate, without energy expenditure from outside, i.e., due to its own heat release.

Considerable interest of researchers and technical experts in methods of producing, structure and properties of nanoscale systems is due to the diversity and uniqueness of their practical applications. The small size of the structural components – usually up to 100 nm – determines the difference between the properties of nanomaterials and their analogs with larger particle sizes [6]-[8].

The scientific and engineering area "Nanoparticles – materials, technologies, and devices has emerged in the last decade in many industrial countries, and its funding is the fastest growing in the world. National and multinational companies are engaged in the production of nanomaterials and large-scale studies in this area [7], [8].

The formation of carbon fibers were observed in the pyrolysis of benzene in 1976 [9]. In 1991, carbon nanotubes in an arc discharge of graphite were discovered [10], followed by the rapid development of this field. Due to a unique combination of different properties, carbon nanotubes are of interest for both basic and applied research [11].

Over the past few years, more than 150 papers on self-propagating high-temperature synthesis of nanomaterials were published, a review of which is given in [12]. In SHS, as in powder metallurgy, the particle sizes of reactants significantly affect both the process and the properties of the materials produced [12]. In this regard, the SHS is closely related to nanotechnologies.

This paper presents original results on the development of a technology for producing carbon nanomaterials for various applications obtained at the Institute of Combustion Problems:

- synthesis of fullerenes in flames;
- synthesis of carbon nanotubes in flames;
- synthesis of a superhydrophobic carbon surface in the combustion regime;
- synthesis of graphene in flames;
- SHS of nanoscale materials;
- formation of Al_2O_3 whiskers during SHS in the Al–B_2O_3–Cr_2O_3 system;
- synthesis of nanoscale catalysts for carbon dioxide re-forming of methane to synthesis gas.

Fullerene synthesis in flame

The structure of fullerene C_{60} proposed by R. Smalley resembles a football, so it is sometimes called footballene, and that of C_{70} resembles a rugby ball. Fullerenes C_{60} and C_{70} were identified in 1985 and prepared in macroscopic quantities in 1990, both by evaporation of graphite in an arc discharge [13]. In flames, fullerene ions were found in 1987, and in 1991, C_{60} and C_{70} were extracted in large quantities from laminar sooting flames of premixed mixtures of benzene and oxygen at low pressures [14], [15] and then spectroscopically identified.

It is known that the formation and synthesis of fullerenes in the traditional method of arc evaporation of graphite is performed at pressures $p < 40$ Torr [16].

As noted in [17], nano- and subnanosize particles are formed by gas-phase condensation in asymptotic giant branched stars. Experiments were carried out at pressures of 0.1-2.6 and 7 mbar, close to the values of p in the

This work was supported in part by the state order for the budget program "Grant funding for research" for 2012-2014 y. on "Formation of layered graphene films in the flame", "Obtaining of nanosized superhydrophobic carbon materials in mode pyrolysis and combustion of hydrocarbons", "Improving of the efficiency solar cells using metal oxide nanoparticles and layered graphene films synthesized in the flame"

Zulkhair Aimukhametovich Mansurov, the Institute of Combustion Problems, 172 Bogenbai Batyr, 050012, Almaty, Kazakhstan (corresponding author to provide phone: +7 727 292 43 46; fax: +7 727 292 58 11; e-mail: zmansurov@kaznu.kz).

astrophysical atmosphere at temperatures T < 1 700 K, at which the formation of fullerenes was observed.

Because fullerenes are formed at low pressures, the corresponding spatial orientation is important, which requires a consideration of the steric factor. For a molecule of C_{60} to form, a spatial orientation of two molecules of C_{30} is required. There are various models of formation of fullerenes C_{60}, one of which is the zip mechanism [18] (Fig. 1).

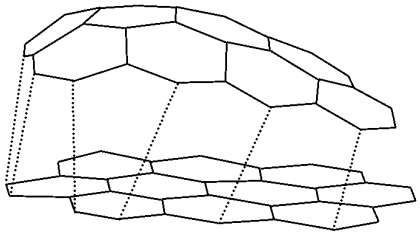

Fig. 1 model of five- and six-membered rings through the connection of two PCAHs by the zip mechanism [18]

A necessary condition for this mechanism is low pressure. As the pressure increases, i.e., with transition to atmospheric pressure or above, where triple collisions dominate, PCAHs coagulate to form soot clusters. It has been shown [15] that the maximum of fullerene formation is shifted to the right relative to the maximum of soot formation. In a detailed study of fullerene formation from benzene flames, the second maximum at 70 mm from the burner matrix was detected [19] (Fig. 2). These data have provided the basis for the development of an alternative method of producing fullerenes in the hydrocarbon combustion regime.

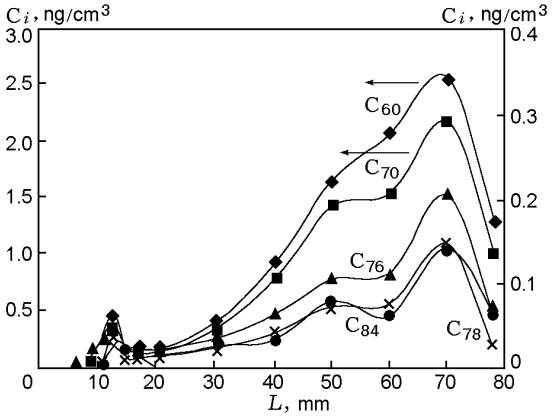

Fig. 2 concentrations profile of fullerenes on the axis of a premixed benzene-oxygen-argon flame [19]

The influence of gas discharge, the type of electrode, and the inter electrode spacing on the yield of fullerenes in combustion was studied in [20]. The experimental conditions were as follows: C/O = 1, p = 40 Torr, flow rate of benzene 250 cm^3/min, oxygen 758 cm^3/min, argon 101 cm^3/min, v = 18.4 cm/s, T = 1200 K, and δ = 0.5-0.8 cm; electrode systems are the needle- plane, plane-plane, and ring-plane with an inter electrode spacing of 4-21 cm; voltage U = 0.5-20 kV. A premixed C_6H_6/O_2/Ar flame under conditions corresponding to the maximum yield of fullerenes was studied [20].

Processing of the experimental data revealed the advantage of the ring electrode over the electrode in the form of a needle and showed that the yield of fullerene C_{60} (≈ 15 %) was the highest when the electrode was placed in the middle of the flame (L = 4 cm).

It has been found [20] that if the peripheral zone of the benzene flame is heated by some external source, such as a laser beam, which not just burns the soot but also creates the same conditions as in the middle of the flame, the concentration of fullerenes increases.

The effect of acetylene-oxygen flames on the different zones along the height of the benzene-oxygen flame have been studied using a ring burner. It has been found that fullerene formation is activated at the boundary of contact of the acetylene-oxygen and benzene-oxygen flames. The positive effect of the acetylene flame consists of increasing the temperature in the upper part of the reaction zone of the main benzene-oxygen flame by 50 ◦C, increasing the degree of ionization, and intense conversion of PCAHs present in the benzene-oxygen flame to fullerenes [21].

Formation of carbon nanotubes in flames

The most promising way to produce carbon nanotubes, according to Merchan-Merchan et al. [22], is the flame method. In the synthesis of carbon nanoparticles using flames, part of the fuel is consumed in heating of the mixture, and part is used as a reactant, which makes this method more cost-effective than methods based on the use of electricity, pyrolysis of hydrocarbons or arc evaporation of graphite.

Results of a study of flat diffusion propane – oxygen flame stabilized on an opposed-jet burner at atmospheric pressure are presented in [23]. Two opposed flows formed the flat flame. The flame was surrounded by an external nitrogen flow supplied from the burner matrices. A solution of catalyst [$Fe(CO)_5$ or an alcoholic solution of nickel nitrate] was sprayed by an ultrasonic nebulizer and delivered through a metal nozzle into the flame from the side of the fuel. The conditions of the experiment are shown in Table 1.

Table 1. Experimental conditions

Catalyst	Flow of catalyst, cm^3/min	Gas flow rate, cm^3/min				Flame temperature,° C
		C_2H_2	O_2	N_2	C_3H_8	
$Fe(CO)_5$	0.05	130-210	100-170	50-200	-	1700-1850
$Ni(NO_3)_2$ *$6H_2O$	0.05	-	160-210	50-200	70-160	900-1150

The resulting products were deposited on the walls of the reactor and collected in traps with liquid nitrogen. The temperature in the reactor was measured by a thermocouple, and in the flame by an Iron Ultrimax pyrometer. It is evident that the samples contain soot agglomerates, among which metal particles are encountered. It was found that under certain

ISBN: 978-1-61804-284-2

experimental conditions, well-ordered bundles of carbon nanotubes 20-30 nm in diameter formed. It is evident from Fig. 3 that the samples contain soot agglomerates, among which metal particles are encountered. It was found that under certain experimental conditions, well-ordered bundles of carbon.

The flame synthesis of carbon nanomaterials is mainly determined by carbon atoms serving as sources of graphite layers, the catalytic metals providing the transformation of the gas-phase carbon atoms into solid graphite layers, and the heat sources activating the catalytic metals.

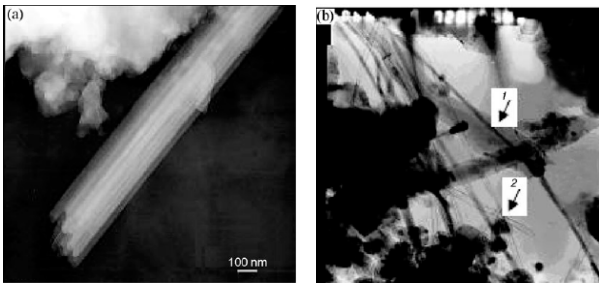

Fig. 3 electron micrographs of samples: (1) carbon nanotube; (2) Ni in a carbon shell

In [24], the synthesis of carbon nanotubes and nanofibres on a $Ni(NO_3)_2$ film deposited on a metal substrate with the use of a counter-flow ethylene flame as a heat source was investigated. Puri et al. have developed, on the basis of numerous experimental data on synthesis of carbon nanotubes in a flame, a model of formation of these nanotubes with participation of nanoparticles of the catalysts (Fe, Ni, Co) [25], [26], [27]. Fig. 4, a schematically described of the CNT formation process and in Fig. 4, b are shown schematic diagram of the CNT growth model by Puri and et al [25]. In this article [25] was underlined that the chemistry includes PAH species but soot was not modeled, since it has negligible presence in the flame.

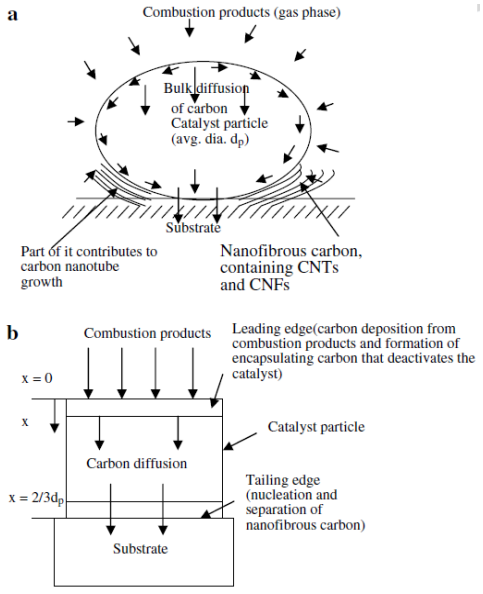

Fig. 4 (a) schematic diagram of the CNT formation process; (b) Schematic diagram of the CNT growth model [25]

In accordance with this model, nucleation of carbon nanotubes begins when the density of carbon atoms on the surface of the catalyst particles increases due to the addition of the indicated atoms from the outer shell of these particles. However, once the nucleation and growth of carbon nanotubes begins, carbon atoms are transported through the nanoparticles mainly due to their diffusion. This diffusion decreases with time because of the decrease in the concentration of the carbon atoms.

Formation of hydrophobic soot in hydrocarbon flames

Low surface-energy materials like amorphous carbon (a-C) films are frequently used to modify surfaces in order to control their wettability. The nanobeads are morphologically similar to the carbon nanopearls synthesized by Levesque and co-workers [28] by acetylene dissociation at 700 ^{0}C on nickel catalyst nanoclusters. Puri et al. [27] have determined new ways of synthesis of carbon nanotubes in the fuel-rich diffusion flames, exposed to an electric field during 2-10 min, on superhydrophobic surfaces representing nanodimensional round amorphous carbon particles deposited on a silicon substrate.

A silicon (Si) disk is placed 2 cm above the burner, as shown in Fig. 5, and exposed to the flame for 4, 6 and 10 minutes. The nonpremixed flame is established using propane and oxygen flow rates of 50-150 cm^3/ min and 260-310 cm^3/min.

Si disc with a carbon nano-bead coating after a 4 min exposure to the flame showing the three deposition zones are shown in Fig. 5, b. The deposited carbonaceous material was examined using Raman spectroscopy. The Raman spectra for the middle zone indicate the presence of several modifications of carbon. Raman peaks near 1350 cm^{-1} (D - amorphous) and 1590 cm^{-1} (G - graphite) in all three zones (1-3). The peaks near 1470 cm^{-1} for Zones 1 and 2 are typical of fullerenes [29].

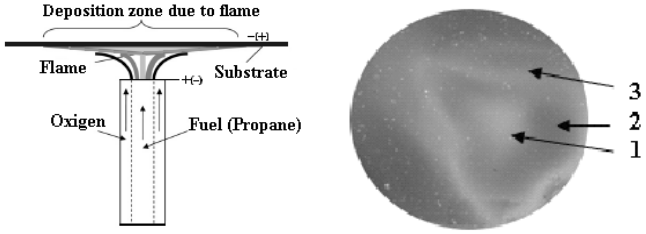

Fig. 5 schematic representation of the burning experimental setup (a) and Si disc with a carbon nanobead coating after a 4 min exposure to the flame showing the deposition zones (b)

The formation of hydrophobic soot surface on silicon and nickel substrates during combustion of propane-oxygen flame was studied [29]. It is stated that the hydrophobic properties are due to the presence of soot particles in the form of nanobeads.

Fig. 8 shows a drop water on a hydrophobic surface, and, as we found, the hydrophobicity of the surface was very stable. The outer contact angle θ is in the range of 152.4–157.1˚ in all cases.

ISBN: 978-1-61804-284-2

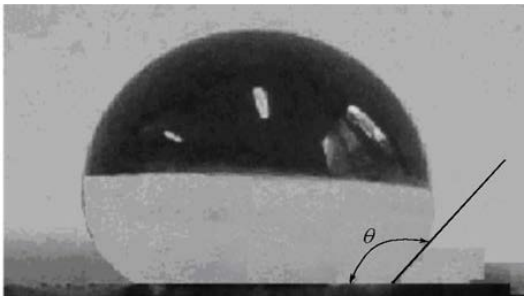

Fig. 8 a liquid drop on the superhydrophobic surface

It was investigated the influence of an electric field of 1 kV applied between the substrate and the burner rim. For studies the substrates were exposed with and without the applied field, in both cases for 10 minutes, to a flame established at propane and oxygen flow rates of 50 and 260 cm^3/min. For this flame, shown schematically in Fig. 5, middle zone contained carbon nano-bead chains that were 15 - 30 nm long in the absence of an electric field. The chain length was increased to 40-50 nm in middle zone when the electrical field was applied. In the outer zone, regardless of the conditions of combustion, there are coagulated aggregates of soot particles with sizes 30-50 nm.

The results for the exploration of the soot formation of hydrophobic surfaces on silicon and nickel substrates during combustion of propane oxygen flame are listed. The distance from the matrix burner and the substrate was varied, the exposure time and the influence of an electric field of different polarity and voltage. It is shown that at the exposure of more than 4 minutes the soot with hydrophobic properties is formed and division of the soot surface area is occurred. The applying of an electric field narrows the soot deposition on the substrate and in diameter of 2.5-3 cm from the center, the soot super hydrophobic surface with a wetting angle of more than 170 ° is formed [30], [31].

Formation of a layered graphene films in the flames [32]

Synthesis graphene in the flame was conducted at a pressure of 40-100 Torr by combustion premixed butane-oxygen mixture with the addition of benzene on a nickel substrate. For this purpose, the burner was placed in a quartz reactor (Fig. 6, a), which created initial low pressure of 5 Torr. The experiments were performed in the following conditions: butane flow rate of 450 cm^3/min, oxygen flow rate of 740 cm^3/min and benzene flow rate of 70 – 120 cm^3/min corresponding to the C/O ratio = 0.8-0.9. Nickel plate was used as the catalyst substrate. The flame temperature in the experiments was in the range of 900-950 ^oC. The residence time of the plate in the flame was 3 min. Fig. 6 shows the photograph of quartz reactor (a) and photo of the flame with the insert of a nickel substrate (b).

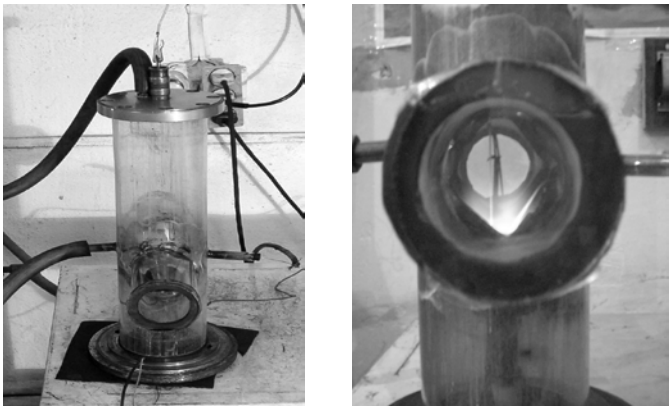

a b

Fig. 6 the photograph of the burner used for low-pressure synthesis of graphene layers in the flame: a – general view, b – with the substrate placed in the flame

Investigations on synthesis of graphene layers in hydrocarbon flame at low pressure have shown that the formation of graphene layers is occurred in sooting zone as well as at atmospheric pressure, as was shown in [32]. Fig. 7 shows the Raman spectra (a) that characterizing the carbon structures are formed on nickel plate in areas 0, 1, 2, 3 (b). In zones 0, 1 and 2 (Fig. 7, a, b) the amorphous carbon structure is observed, but in zone 3 the graphene layers are synthesized. At that, an area of graphene formation at low pressure is more expanded than at atmospheric pressure. Above zone 3 there is soot structure is formed (Fig. 7, b).

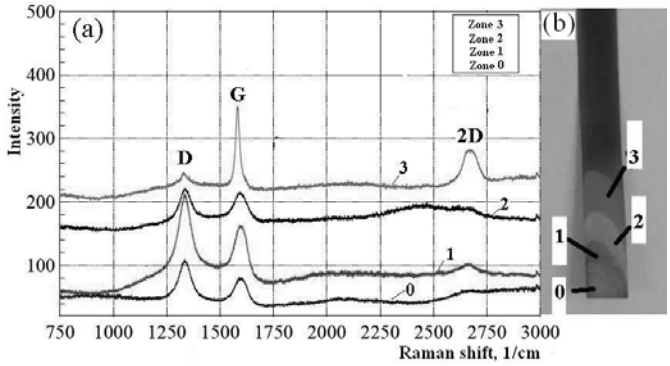

Fig. 7 the Raman-Spectra of carbon structures in accordance with (a) zones; and photo of nickel substrate (b) with an indication of formed carbon structure zones
(P = 90 Torr, C/O = 0.8, T = 900 °C, t = 30 sec) [33]

Analysis of the results of synthesis of graphene layers in the flame at low pressure and with addition of benzene showed that in the pressure range of 40-100 Torr one- to three-layer graphene sheets on nickel substrate are formed, which is characterized by the intensity ratio $I_G/I_{2D} \leq 1.3$. At a pressure of 55 Torr preferential formation of a single layer graphene is observed, its characteristic Raman spectra was shown in Fig. 8.

ISBN: 978-1-61804-284-2

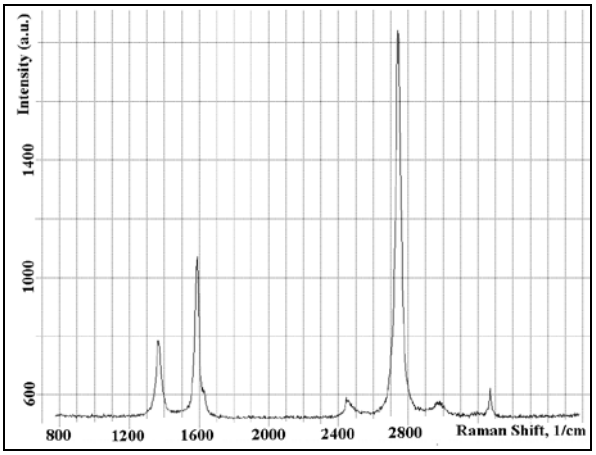

Fig. 8 raman spectra of single-layer graphene samples obtained with the addition of benzene to C_4H_{10}/O_2 flame on a nickel substrate at a pressure of: 55 Torr (I_G/I_{2D} =0.58) [34]

Mechanism of soot formation in rich flames [35]

The flame front structure of soot formation flames can be considered in close connection with mechanism of fuel conversion. A scheme that suggested by Bockhorn [36] in 1994 is known, where polycyclic aromatic hydrocarbon (PAH) are precursors of soot particles. Since then, in rich fuel flames the nanosized particles such as fullerenes and graphenes are found.

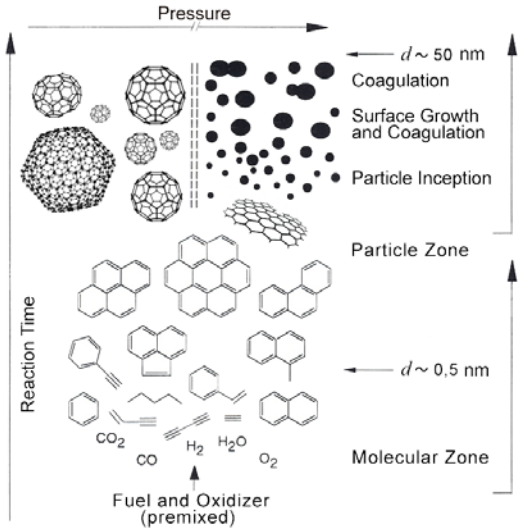

Fig. 9 modified scheme for soot, fullerenes and graphene formation process in flame [35]

The fullerenes formation is generally observed at pressures below 60 Torr, because for fullerenes formation is necessary an adherence of steric spatial factor, but in flames at atmospheric pressure this factor is pre- vented by triple collisions. Therefore, the pressure coordinate can be introduced to the general scheme for soot formation. At low pressure the formation of fullerenes from polycyclic aromatic hydrocarbon (PAH) is occurred, but with pressure increase the polycyclic aromatic hydrocarbon (PAH) is coagulates to soot particles. From (PAH) follows the graphene formation as intermediate product between PAH and soot particles, which is confirmed by the formation of multi-layered graphene films at atmospheric pressure and single-layered at the pressures below 60 Torr. On the basis of the data on synthesis of fullerenes, carbon nanotubes, superhydrophobic soot and graphene in the flame it is possible to modify the general scheme proposed by H. Bockhorn [36] for rich fuel flames, namely to make a pressure-coordinate, which allows the formation of fullerenes at low pressures, and soot at high pressures. In addition the scheme was completed by graphene formation as an intermediate product stage of graphene formation (Fig. 9) [35].

Increase of the power of solar cells coating by nanoparticles of nickel oxides synthesized in flame

The work present the investigations results on synthesis of nickel oxide nanoparticles in propane-oxygen flame in counter jets which subsequently are used to increase the efficiency of light conversion in the solar cells.

The reactor of the burner is a hollow cylinder with a diameter of 150 mm and a height of 82 mm is made of stainless steel. Two burners are installed on the axis of this cylinder opposite each other. Nichromic wire with a diameter of 0.3 mm was used as a substrate for the growth of nickel oxide nanoparticles. X-ray fluorescent analysis of nichromic wire shows that the main composition wire is Ni-60.27 %. The wire before its using for synthesis of nanoparticles was preliminary treated with 25 % solution of nitric acid for 20 minutes [37].

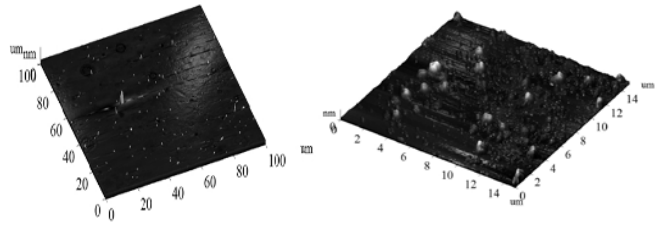

Fig. 10 photo of nickel oxide nanoparticles on the surface of the solar cell, 5sec (a) 2 min (b) [37]

The obtained results of electron-microscopic investigations show that the treatment of nichromic wire with flame for 2 minutes leads to the formation of nickel oxides with an average size of 300 nm on its surface. High temperature and active radicals formed in propane-oxygen flame interact with nickel surface promoting the growth of nickel nanoparticles. After coating of nickel oxide nanoparticle were on the surface of solar cell on atomic power microscope. The resulting image (Fig. 10) shows that the size of metal oxide nanoparticles on the surface of a solar cell depends on the residence time in the flame [38].

To study output characteristics silicon solar cells with an active region of 1 cm^2 were used. To obtain uniform coating based on nanoparticles on the surface of the solar cell suspension of nanoparticles was preliminary created in ethanol

in ultrasonic bath. To coat one solar element up to 0.1 ml of suspension was necessary. Primordially the measurement of short – circuit current and voltage of non-load running of the solar element without applying a coating was carried out. Not changing the conditions of the experiment short-circuits current and open circuit voltage with applied nanooxide film was measured.

The applying of silicon solar cells of nickel oxide nanoparticles to the surface caused the increase of output open circuit voltage of 4-7 %, the increase of short – circuit current of 2-8 %, that in total caused the increase of efficiency of the solar cells by 2-3 % [38].

SHS of nanoscale materials

Producing a silicon nanopowder is an important problem for various applications, including microelectronics, solar power engineering, and rocket propellants. In [39], a silicon nanopowder was produced by SHS, which is a simple and cost-and power-effective technology for producing various materials. The principal possibility of producing a pure silicon powder with a high surface area is shown, and a comparative analysis of the products obtained using three different silicon oxides was made.

The method is based on the well-known process of magnesium-thermic reduction of silica but which is carried out in the regime of a self-propagating combustion reaction. The starting material was silicon oxide powders differing in particle size and purity: quartz of the Erken Kazakhstan field (hereinafter in the text, quartz KZ) with a purity 98.8% and a particle size $d \leq 100$ μm; Cerac quartz (WI, USA) with a purity 99.9% and a particle size of $d < 44$ μm; untreated fumed silica (UFS) qurtz (Cabot Corporation, MA, USA) with a purity of 99.9% and a specific surface of ≈ 200 m^2/g.

Synthesis was carried out by the following reaction:

$$SiO_2 + 2Mg = Si + 2MgO \quad (1)$$

The synthesized samples were treated with 36 % hydrochloric acid for 3 hours under normal conditions to produce pure silica. It is evident from Fig. 11 that the typical microstructure (morphology and size) of the synthesized silicon powder depends weakly on the morphology and particle size of the initial quartz. In all cases, the powder has a very porous microstructure with a particle size of the components (pores and separate crystallites) not less than 1 μm.

Due to rapid cooling, the microstructure of the product consists of small (≤ 1 μm) MgO grains a silicon matrix. Chemical removal of MgO yielded a very porous silicon skeleton with a typical size of the microstructure comparable to the scale of the grain size of magnesium oxide crystals. The size of these grains is determined solely by the rate of crystallization and temperature conditions in the combustion wave (most likely, the rate of cooling of the product). A weak dependence of the microstructure of the synthesized silicon on the size of SiO_2 was observed.

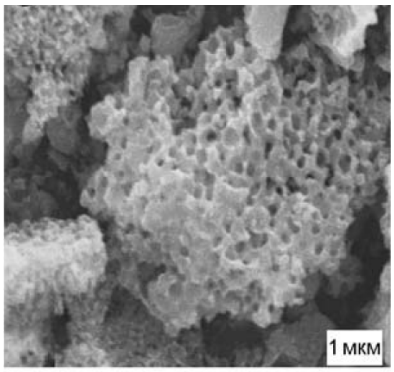

KZ

Fig. 11 particles of synthesized silicon after chemical treatment with hydrochloric acid

Since the silicon produced in all cases has a highly porous, sponge-like structure with high surface area, it is reasonable to assume that a fine (submicron or nanosized) silicon powder can be obtained by mechanically destroying the thin bridges of the skeleton. Treatment in a high-energy mill (Glen Mills Inc., USA) for 5 min resulted in a submicron silicon powder with a particle size of 300 nm.

SHS of Al_2O_3 whiskers in the $Al–B_2O_3–Cr_2O_3$ system

In [40], SHS was performed in the $Cr_2O_3–B_2O_3–Al$ and $Cr_2O_3–B_2O_3–Mg$ systems.

Borides of chromium and aluminum oxide were identified by x-ray diffraction analysis. It is seen that a small portion of aluminum interacted with air to give AlN.

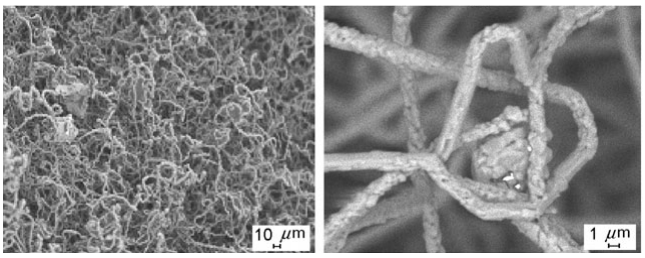

a b

Fig. 12 sem images of the $Cr_2O_3 –B_2O_3–Al$ system: (a) straight, wavy, and twisted forms of whiskers; (b) branching of several crystals

Results of an electron microscopic study of the combustion products of Cr_2O_3-B_2O_3-Al indicate the formation of whiskers of different sizes and shapes from aluminum oxide in a boride matrix (Fig. 12). Fig. 12 a shows fibers of straight, twisted, and wavy forms, and Fig. 12 b shows whiskers with a branched structure. Analysis on a scanning electron microscope (SEM) revealed the formation of α-Al_2O_3 fibers with a length $l \approx$ 10-25 μm and a diameter d = 200-500 nm. The fibers are not ordered. Different fiber diameters are

due to self-turbulence in the growth of the system, namely, in the growth in temperature, diffusion, and chemical reaction rate [39]. The process of formation and the mechanism of growth of aluminum oxide whiskers and fibers were studied in [41]-[43]. Aluminum, as follows from the literature, can serve as a concentrator of whisker growth by the vapor–liquid–crystal mechanism.

Synthesis of nanoscale catalysts for carbon dioxide reforming of methane to synthesis gas

Fiber glass-based metal oxide (CoO and NiO) catalysts were developed. Use was made of KS-11-LA (88) Na–Si fiberglass (the working temperature range of this fiber glass is 1000–1200 ◦C). Oxides of metallic Ni and Co were deposited on its surface by solution combustion (SC) [44] which is a version of self-propagating high- temperature synthesis [45], [46].

Samples with a low content of oxides – not more than 1% by weight were synthesized (IK1–IK5 in Table 2).

A fiber-glass sample of size 5 × 5 cm was impregnated with a solution of nitrate salts of cobalt, nickel, and glycine taking into account its water capacity, and the sample was then dried for 30 min in air at 100 ◦C.

Table 2. Synthesis conditions of fiberglass catalysts

Sample number	*C*cat, %	Co/Ni, %	Glycine, mol
IK1	1.0	100/0	4.0
IK2	1.0	70/30	4.0
IK3	1.0	50/50	4.0
IK4	1.0	30/70	4.0
IK5	1.0	0/100	4.0

As shown by physicochemical studies, the formation of 10–50 nm nanoparticles occurred during heating of samples in a thermostatic oven at 400–450 ◦C for 1 h, followed (in the case of using a ≥1% concentration of the active ingredient) by weak bluish glow.

The method of SC between the starting components corresponds to the reaction:

$$Me(NO_3)_2 \cdot nH_2O + 4C_2H_5NO_2 + 2.5O_2 = 8CO + 16H_2O + 3N_2 + MeO,$$

where $C_2H_5NO_2$ is glycine, which acts as a reducing agent. Additional missing oxygen comes from the air.

Investigation of the surface of the fiber-glass sample by SEM and TEM (transmission electron microscope) revealed that the active component is dispersed mainly in the form of individual particles with a size of about 10 nm or less, which form an oxide film.

Fig. 13 (a) shows a three-dimensional image of individual particles of the 1.0-KS-0/100 catalyst taken from the substrate using an ultrasonic disperser.

A TEM image of the 0.8-KT-60/40 catalyst Fig. 13 (b) showed the presence of cobalt and nickel particles with a size of 5-20 nm on the fiber-glass surface.

In connection with the annual decline of oil reserves in the world, there is an urgent need for new sources of alternative clean fuel. Such a fuel can be dimethyl ether produced from synthesis gas by carbon dioxide reforming of methane. Among the investigated catalytic systems used in the carbon dioxide reforming of methane and other hydrocarbons are deposited nickel (Ni/Al_2O_3, Ni/SiO_2, and Ni_3Al) and cobalt-nickel catalysts, code- posited Ni–Mg contacts (Ni0.03Mg0.97O), and catalysts based on precious metals.

Dependences of the conversion of the starting sub- stances, methane, carbon dioxide, and the yield of the desired reaction products (hydrogen and carbon monoxide) on the temperature and time of catalysis have been studied. The IK1 catalyst showed rather high activity: the yield of synthesis gas reaches 32 % H_2 and 46 % CO at 745 ◦C. The conversion of CH_4 is 30 %, and that of CO2 is 80 % at the same temperature.

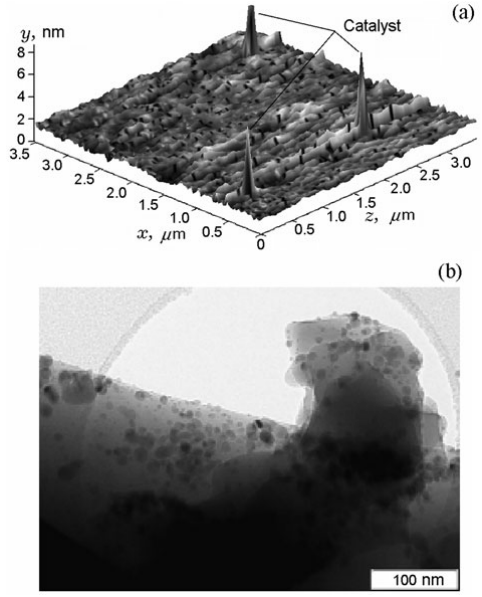

Fig. 13 three-dimensional image of particles of the 1.0-KC-0/100 catalyst (a) obtained in an atomic force microscope and a TEM image of the 0.8-KT-60/40 catalyst (b)

Samples of catalysts coated with cobalt oxide exhibit high activity in the carbon dioxide reforming of methane. It should be noted that compared to the GIAP-18 commercial catalyst, the IK1 fiber-glass catalyst is carbonized much slower, and after 3 h of operation, the degree of carbonization of IK1 did not exceed 0.5%.

CONCLUSIONS

It was established the formation of fullerenes and carbon nanotubes as well as soot with the superhydrophobic surface,

ISBN: 978-1-61804-284-2

obtained on nickel and silicon supports in benzene-oxygen and propane-oxygen diffusion flames. New results regarding the synthesis of superhydrophobic surface with a contact angle 135-175 ° have great practical interest as anti-corrosion additives to various materials. Graphene sheets with 1-3 layers are mainly formed in the range of 40-100 Torr on nickel substrate in butane-oxygen flame with the addition of benzene. At pressure of 45-55 Torr preferential formation of a single layer graphene is observed.

The photovoltaic properties of solar cells coated by nickel oxide nanoparticles synthesized in counter flow propane-air flame. It is revealed that coated the surface of a silicon solar cell by nickel oxide nanoparticles results in the increase in solar cell efficiency by 3%.

SHS of nanopowders of metal oxides and catalysts is an alternative to the conventional technology of producing inorganic substances and materials.

All these processes are characterized by the use of the chemical energy of combustion instead of electric energy; ease of equipment due to the absence of external sources of heat; and a high rate of the process.

REFERENCES

1. N. N. Semenov, Some Problems of Chemical Kinetics and Reactivity (Izd. Akad. Nauk SSSR, Moscow, 1954 [in Russian].

2. Ya. B. Zel'dovich, G. I. Barenblatt, V. B. Librovich, and G. M. Makhviladze, Mathematical Theory of Combustion and Explosion (Nauka, Moscow, 1980; Plenum, New York, 1985).

3. D. A. Frank-Kamenetskii, Diffusion and Heat Transfer in Chemical Kinetics (Nauka, Moscow, 1967; Plenum, New York, 1969).

4. G. I. Ksandopulo and V. V. Dubinin, Gas-Phase Chemistry of Combustion (Khimiya, Moscow, 1987) [in Russian].

5. A. G. Merzhanov, "Combustion and Explosion in Physical Chemistry and Technology of Inorganic Materials," Usp. Khim. 72 (4), 323–345 (2003).

6. K. E. Drexler, Nanosystems: Molecular Machinery, Manufacturing and Computation (John Wiley and Sons, New York, 1992). Nanotechnologies. Nanomaterials. Nanosystem Equipment. Global Progress Ed. by P. P. Mal'tsev (Tekhnosphera, Moscow, 2008 [in Russian].

7. W. F. Smith and J. Hashemi, Foundations of Materials Science and Engineering (McGraw-Hill, 2010).

8. A. Oberlin, M. Endo, and T. Koyama, "Filamentous Growth of Carbon Through Benzene Decomposition," Cryst. Growth 32 (3), 335–349 (1976).

9. S. Iijima, "Helical Microtubules of Graphitic Carbon," Nature 354, 56–58 (1991).

10. M. Endo, M. S. Strano, and P. M. Ajayan, Potential Applications of Carbon Nanotubes, Eds. by A. Jorio, G. Dresselhaus, M. S. Dresselhaus (2008), pp. 13–61. (Topics in Appl. Phys., Vol. 11.)

11. Z. A. Mansurov, "Some Applications of Nanocarbon Materials for Novel Devices," in Nonoscale-Devices—Fundamentals, Ed. by R. Gross et al. (Springer, 2006), pp. 355–368.

12. A. E. Sychev and A. G. Merzhanov, "Self-Propagating High-Temperature Synthesis of Nanomaterials," Usp. Khim. 73 (2), 157–170 (2004).

13. H. W. Kroto, J. R. Health, S. C. O'Brien, R. F. Curl, and R. F. Smalley, "C60 : Buckminsterfullerene," Nature 318 (6042), 162–164 (1985).

14. J. B. Howard, "Fullerenes Formation in Flames," in 24th Symp. (Int.) on Combustion (1992), pp. 933–946.

15. W. Kra¨tschmer, L. Lamb, K. Fostiropoulos, D. Huffman, "Solid C: A New Form of Carbon," Nature 347, 354–358 (1990).

16. C. J¨ager, F. Huisken, Jansa I. Lamas, Th. Henning, "Formation of Polycyclic Aromatic Hydrocarbons and Carbonaceous Solids in Gas-Phase Condensation Experiments," Astrophys., No 696, 706–712 (2009).

17. J. Ahrens, M. Bachmann, Th. Baum, J. Griesheimer, R. Kovacs, P. Weilmu¨nster, K.-H. Homann, "Fullerenes and Their Ions in Hydrocarbon Flames," Int. J. Mass Spectrom. Ion Proc. 138, 133–148 (1994)

18. W. J. Grieco, A. L. Lafleur, K. C. Swallow, et al. "Fullerenes and PAH in Low-Pressure Premixed Benzene/Oxygen Flames," in Symp. (Int.) on Combustion 27 (2), 1669–1675 (1998)

19. Z. A. Mansurov, N. G. Prikhodko, T. T. Mashan, and B. T. Lesbaev, "The Study of Influence of Electric Field on Soot Formation at Low Pressure," Chem. Physics 25 (10), 18–22 (2006)

20. M. Bachman, W. Wiese, and K.-H. Homann, "Thermal and Chemical Influences on the Soot Mass Growth," in Symp. (Int.) on Combustion 25 (1), 635–643 (1994)

21. N. G. Prikhod'ko, "Features of Formation of Fullerenes and Nanotubes in Combustion of Hydrocarbons in an Electric Field," Doct. Dissertation in Chem. Sci. (Al- Farabi Kazakh National University, Almaty, 2010)

22. W. Merchan-Merchan, A. V. Saveliev, L. A. Kennedy, "High-Rate Flame Synthesis of Vertically Aligned Car- bon Nanotubes using Electric Field Control," Carbon 42, 599–608 (2004)

23. D. I. Chenchik, Z. A. Mansurov, T. A. Shabanova, and T. Orynshaikh, "Producing Carbon Nanotubes in an Opposed-Jet Burner," in Int. Symp. Combustion and Plasma Chemistry (Almaty, 2007), pp. 288–290

24. G. W. Lee, J. Jurng, and J. Hwang, Formation of Ni-catalyzed multiwalled carbon nanotubes and nanofibers on a substrate using an ethylene inverse diffusion flame, J. Combust. Flame, 139, 167–175 (2004).

25. S. Naha, S. Sen, A. K. De, and I. K. Puri, A detailed model for the flame synthesis of carbon nanotubes and nanofibers, Proc. Combust. Inst., 31, Issue 2, 1821–1829 (2007).

26. S. Naha and I. K. Puri, A model for catalytic growth of carbon nanotubes, J. Phys. D: Appl. Phys., 41, No. 065304, 6

(2008).

27. S. Naha, S. Sen, and I. K. Puri, Flame synthesis of superhydrophobic amorphous carbon surfaces, J. Carbon, 45, Issue 8, 1702–1706 (2007).

28. A. Levesque, V. T. Binh, V. Semet, D. Guillot, R. Y. Filit, M. D. Brookes, et al., "Mono Disperse Car- bon Nanopearls an a Foam-Like Arrangement: A New Carbon Nano-Compound for Cold Cathodes," Thin Solid Films, Nos. 464 and 465, 308-314 (2004)

29. M. Nazhipkyzy, Z. A. Mansurov, I. K. Puri, T. A. Shabanova, and I. A. Tsyganova, "Producing a Super- hydrophobic Carbon Surface during Propane Combus- tion," Neft Gaz 5 (59), 27–33 (2010)

30. Mansurov Z.A. Soot and nanomaterials synthesis in the flame// Journal of Materials Science and Chemical Engineering. 2014, 2, P.1-6

31. Innovative patent of the Republic of Kazakhstan № 26912. Method for producing a hydrophobic carbon black. Published in BI 2013, № 5.

32. Prikhodko, N.G., Lesbayev, B.T., Auyelkhankyzy, M., Mansurov, Z.A. Synthesis of Graphene Films in a Flame//Rus. J. of Phys. Chem. B, 2014. 8, 1. P. 61–64.

33. Prikhodko N.G., Auyelkhankyzy M., Lesbayev B.T., Mansurov Z.A. Combustion synthesis of graphene films // 35th Intern. Symposium on Combustion 2014. – San Francisko, California, USA, 2014.

34. Prikhodko N.G., Auyelkhankyzy M., Lesbayev B.T., Mansurov Z.A. The Effect of Pressure on the Synthesis of Graphene Layers in the Flame // Journal of Materials Science and Chemical Engineering. - 2014. – V. 2, № 1 – P. 13-19.

35. Zel'dovich Memorial: Accomplishments in the combustion science in the last decade / [Edited by A.A. Borisov and S.M. Fialkov]. – Moscow: TORUS PRESS, 2014. – Vol. 1. 196 p. (Mansurov Z.A. From cool flame to nanomaterials synthesis in flames, PP. 17-25)

36. H. Bockhorn (ed). Soot formation in Combustion. Springer-Verlag, Berlin, Heidelberg. 1994. P.4.

37. Innovative patent Republic of Kazakhstan № 27091. Method manufacturing a solar cell. Published in BI 2013, № 6.

38. Lesbayev B.T., Prikhodko N.G., Mansurov Z.A., Auyelkhankyzy M., Chenchik D.I., Dikhanbayev K., Taurbayev T.I., Saveliev A.V. Increase of the Power of Solar Elements Based on Nanoparticles of Nickel Oxides Synthesized in Flame // Advanced Materials Research. 2012. Vol. 486. pp. 140-144.

39. Zh. Yermekova, Z. Mansurov, A. S. Mukasyan, "Combustion Synthesis of Silicon Nanopowders," Int. J. Self-Propag. High-Temp. Syn. 19 (2), 96–103 (2010)

40. D. C. Abdulkarimova, I. M. Vongai, Z. A. Mansurov, and O. Odavara, "Producing Boride Composites by SHS," in Int. Symp. Physics and Chemistry of Carbon Materials/Nanoengineering (Almaty, 2010), pp. 116–118

41. H. Chen, Y. Cao, X. Xiang, J. Li, C. Ge, "Fabrication of β-Si3 n4 Nano-Fibers," J. Alloys Compounds 325 (1, 2), L1–L3 (2001)

42. P. L. Longland, A. I. Moulson, "The growth of α- and β-Si3 N4 Accompanying the Nitriding of Silicon Powder Compacts," J. Mater. Sci 13 (10), 2279–2280 (1978)

43. V. Valc´arcel, A. Souto, F. Guiti´an, "Development of Single-Crystal α-Al2 O3 Fibers by Vapor–Liquid–Solid Deposition (VLS) from Aluminum and Powder Silica," Adv. Mater 10 (2), 138–140 (1998)

44. G. G. Aldashukurova, N. V. Shikina, A. V. Mironenko, Z. A. Mansurov, Z. R. Ismagilov, "Catalysts for Process- ing Light Hydrocarbon Raw Stock: Combustion Syn- thesis and Characterization," Int. J. Self-Propag. High- Temp. Syn. 20 (2), 124(4) (2011)

45. A. S. Mykasyan, P. Dinka, "Novel Approaches to Solution—Combustion Synthesis," Int. J. Self-Propag. High-Temp. Syn. 16 (1), 23–35 (2007)

46. B. M. Reddy, G. K. Reddy, I. Ganesh, M. F. Ferreira Jose, "Single Step Synthesis of Nanosized CeO2—Mx Oy Mixed Oxides (MxOy = SiO2, TiO2 , ZrO2, and Al2 O3) by Microwave Induced Solution Combustion Synthesis: Characterization and CO Oxidation," J. Mater. Sci. Lett. 44 (11), 2743–2751 (2009)